Journal of The Electrochemical Society, **153** (3) B90-B96 (2006)
0013-4651/2006/153(3)/B90/7/$20.00 © The Electrochemical Society

Formation of Phosphate/Permanganate Conversion Coating on AZ31 Magnesium Alloy

C. S. Lin,[a,*,z] C. Y. Lee,[b] W. C. Li,[a] Y. S. Chen,[b] and G. N. Fang[b]

[a]*Department of Materials Science and Engineering, National Taiwan University, Taipei 106, Taiwan*
[b]*Department of Mechanical and Automation Engineering, Da-Yeh University, Changhua 515, Taiwan*

The properties of conversion coating on magnesium can be closely related to its microstructure and composition. This study investigated the evolution and microstructure of phosphate/permanganate conversion coating on AZ31 magnesium alloy. Results show that increasing the solution temperature reduced the growth rate of the coating. The temperature effect lies in the different structure associated with the coating layer contacting the substrate: a porous layer mainly composed of magnesium, aluminum hydroxides/phosphate formed in the solution at 40°C, while a compact magnesium oxide layer formed in the solution at 80°C. The formation mechanism of phosphate/permanganate coating was discussed in detail, with emphasis on the effect of the solution temperature.
 [DOI: 10.1149/1.2164787]

Manuscript submitted June 23, 2005; revised manuscript received November 29, 2005. Available electronically January 25, 2006.

Magnesium alloys have been one of the most highly promising materials employed for high specific strength and stiffness applications such as electrical appliance and automobile parts. Most magnesium alloys, however, tend to suffer severe corrosion during service. Surface modification layers are, therefore, indispensable for improving their corrosion resistance. Such layers can also enhance the adhesion of subsequent painting. Among the various surface modification treatments, chromate conversion treatment has received considerable attention over the years because of its simplicity in the coating process and the excellent corrosion protective properties of the resulting coating.[1-8] Environmental concerns about the use of hexavalent chromate have, however, stimulated the development of nonchromate solutions for the conversion treatment of magnesium alloys, leading to the emergence of phosphate/permanganate,[9-12] stannate,[13-15] and solutions containing salts of rare earth metals[16-19] or cobalt.[20]

Stannate conversion treatment is usually performed in alkaline solutions, in which the coating nucleates on a corrosion film intimately contacting the magnesium substrate.[13,14] The corrosion film exhibits a porous structure,[15] while the coating layer is composed of hemispherical particles developed by a nucleation and growth process. Furthermore, this coating process is strongly influenced by the composition and microstructure of base magnesium alloys[13,14] and the composition and temperature of the solution.[15] The solutions containing salts of rare earth metals in the form of nitrate, sulfate, and chloride are generally used as acid media, among which the one composed of Ce^{3+} has received the most attention. Cerium conversion coating on magnesium has a relatively complex structure that is strongly influenced by the composition of the solution and pretreatments prior to immersion.[17-19] Pre-etching in hydrochloric acid was followed by multiple-step immersions in the cerium chloride solution with addition of hydrogen peroxide; the coating on AZ91 and AM50 alloys was found to consist of two layers, with the major overlay being primarily magnesium/cerium oxides and hydroxides.[18] In contrast, the conversion coating formed on a mechanically polished AZ31 alloy in the cerium nitrate solution comprises three layers: a porous layer mainly consisting of magnesium hydroxide/oxide as an under layer intimately contacting the magnesium substrate, a rather compact layer as intermediate layer, and a fibrous layer as the major overlay.[19] The latter two layers have a similar composition. Both are likely the magnesium/cerium hydroxides.

Unlike the conversion coatings formed in the stannate solution and those containing salts of rare earth metals, the microstructure of phosphate/permanganate conversion coatings is less well studied, although they can exhibit corrosion protective properties comparable to the chromate coating.[9-12] Furthermore, detailed microstructure of the various conversion coatings can help the development of new nonchromate baths for magnesium alloys. This study, therefore, aims at detailing the microstructure and growth behavior of the coating on AZ31 magnesium alloy in phosphate/permanganate solutions at 40 and 80°C.

Experimental

Conversion coating treatment.— The material used in this study is the commercial AZ31 plate that consists of 3.47% (in weight percentage) Al, 1.03% Zn, 0.50% Mn, 0.03% Fe, 0.003% Cu, 0.001% Ni and Mg in balance, as measured by inductively coupled plasma–atomic emission spectrometry (ICP-AES). The coupons with a size of 50 × 20 × 2 mm were mechanically polished using emery paper up to 2400 grit, rinsed with deionized water, cleaned in acetone ultrasonically, and finally dried in a stream of hot air. The plates were then immersed in the solution composed of 20 g L^{-1} potassium permanganate ($KMnO_4$) and 100 g L^{-1} ammonium phosphate ($NH_4H_2PO_4$) at 40 and 80°C, respectively. The pH of the solution was adjusted to be 3.5 via the addition of phosphoric acid or potassium hydroxide. The immersion time was varied from 0.5 to 10 min for investigating the evolution of the coating. After immersion, the plates were thoroughly rinsed in deionized water and then left for drying in room-temperature air overnight.

Microstructural characterization.— The crystallinity and phase of the conversion coating were identified using glancing-angle X-ray diffraction (XRD). The surface morphology of the coating was investigated using a scanning electron microscope (SEM). To prepare cross-sectional transmission electron microscope (TEM) specimens, two AZ31 plates with conversion coatings facing each other were sandwiched together using M-Bond epoxy. The cross-sectional specimens were then prepared using a combined mechanical and ion-beam thinning technique. The TEM specimens were examined via a JOEL JEL3010 analytical TEM. The composition of the coating was measured by energy dispersive spectrometry (EDS) using an electron probe of 10 nm in diameter and the crystal structure was identified by the selected area electron diffraction technique. The thickness of the coating was measured on the cross-sectional SEM or TEM micrographs, and each thickness was reported as an average of at least ten measurements.

Results

Surface morphology of the conversion coating.— Figures 1 and 2 show the evolution of the coating on AZ31 plate immersed in the solution at 40 and 80°C, respectively. A thin layer of coating was visible on the plate immersed in the solution at 40°C for 0.5 min (Fig. 1a). Microcracks were also frequently observed and are marked by the arrow in Fig. 1a. Increasing the immersion time to 2

* Electrochemical Society Active Member.
z E-mail: csclin@ntu.edu.tw

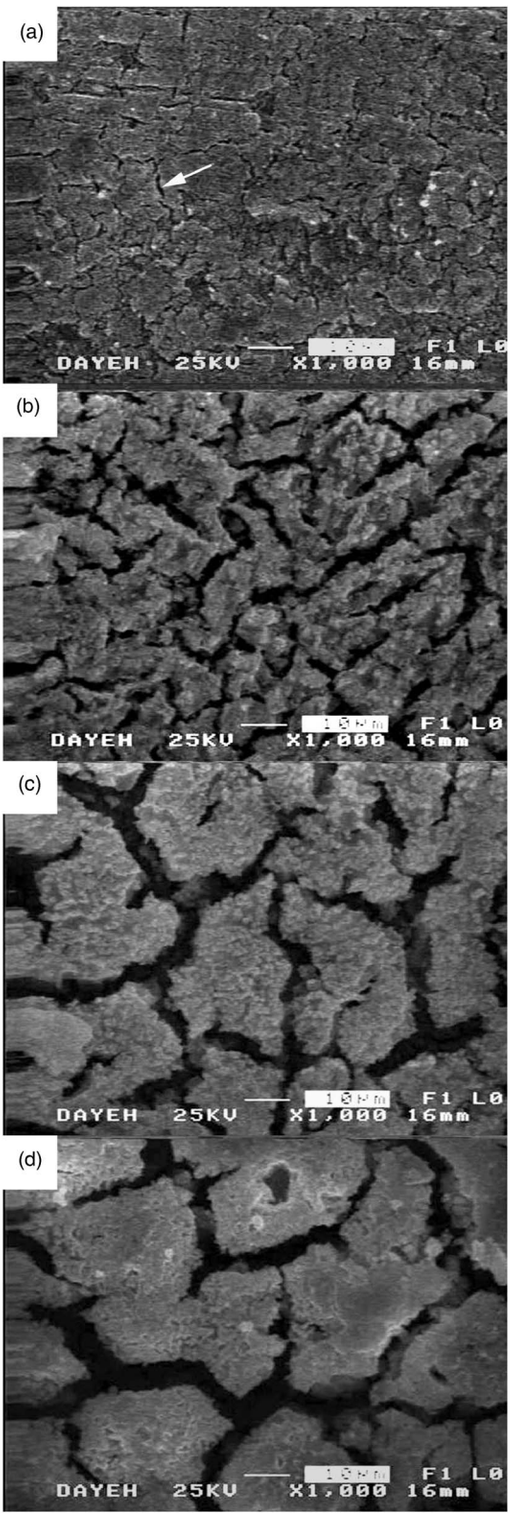

Figure 1. Evolution of surface morphology on AZ31 plate immersed in the phosphate/permanganate solution at 40°C for (a) 0.5; (b) 2; (c) 5; and (d) 10 min.

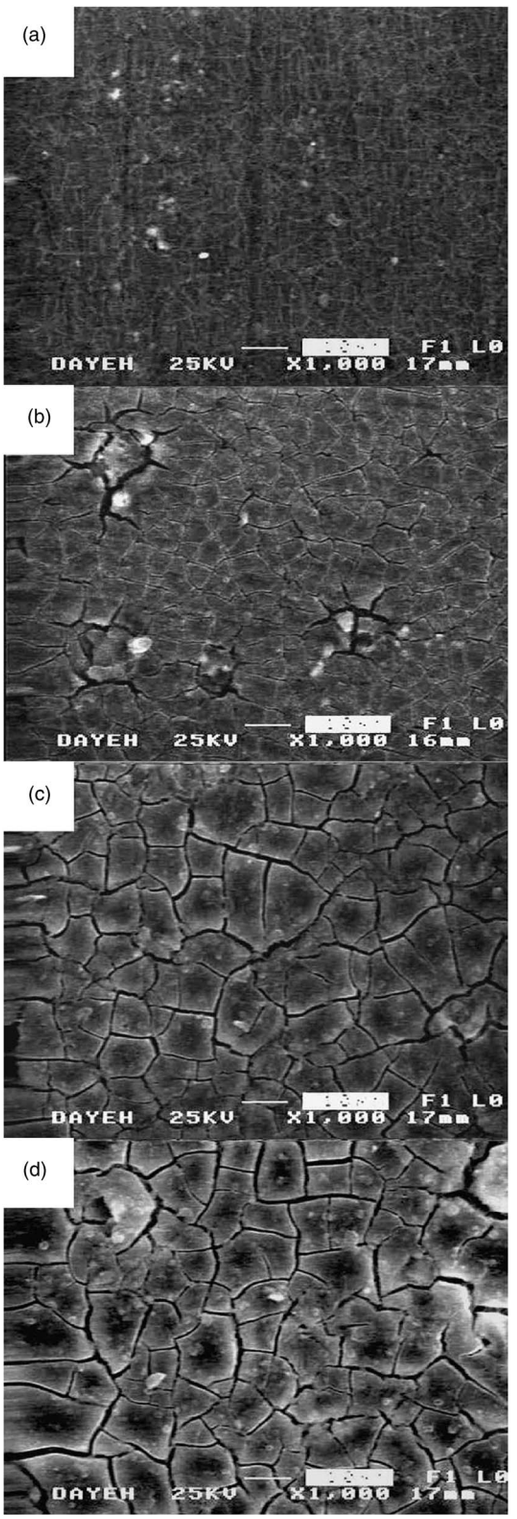

Figure 2. Evolution of surface morphology on AZ31 plate immersed in the phosphate/permanganate solution at 80°C for (a) 0.5; (b) 2; (c) 5; and (d) 10 min.

min resulted in thicker coating and larger microcracks having wider crack openings (Fig. 1b). The coating continued to grow and larger microcracks formed with continued immersion, as shown in Fig. 1c and d. Wider microcracks were apparently associated with thicker coatings, as commonly seen by other researchers studying phosphate/permanganate conversion coating on magnesium.[10-12] These microcracks are partly due to desorption of water during the drying process, because they were hardly observed under an optical

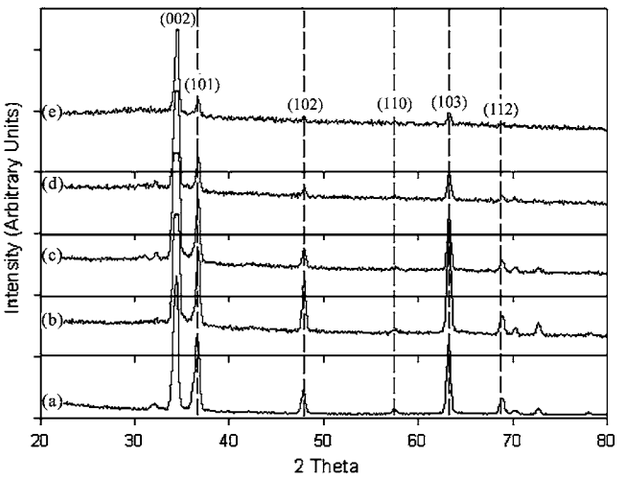

Figure 3. XRD patterns of AZ31 plate (a) without coating and after immersion in the phosphate/permanganate solution at 40°C for (b) 0.5; (c) 2; (d) 5; and (e) 10 min.

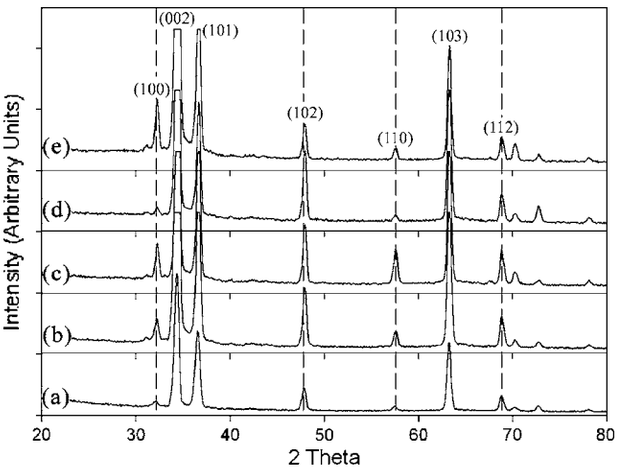

Figure 4. XRD patterns of AZ31 plate (a) without coating and after immersion in the phosphate/permanganate solution at 80°C for (b) 0.5; (c) 2; (d) 5; and (e) 10 min.

microscope at a magnification of 500 immediately after withdrawal of the plate from the solution. Microcracks were observed and became wider late during the drying process.

Figure 2 shows that the plate immersed in the 80°C solution exhibited a similar surface morphology evolution as that in the 40°C solution. Increasing solution temperature, however, markedly reduced the growth rate of the coating because microcracks on the coating formed at 80°C had smaller openings than those formed at 40°C after the same degree of immersion.

XRD analysis.— Figure 3 shows the XRD patterns of the plate with and without the conversion coating formed in the 40°C solution. The pattern of the plate without coating consisted of peaks that can be assigned as those arising from the diffraction of magnesium (Fig. 3a). Other than the peaks corresponding to magnesium, no additional peaks were observed in the plates after various degrees of immersion (Fig. 3b-e). However, the intensity of the peaks from the substrate decreased and the background of the pattern increased with continued immersion. This suggests that the plate might be covered with an amorphous layer that thickened as immersion proceeded. The amorphous phosphate/permanganate conversion coating on magnesium has also been uncovered in the literature.[10-12] The pattern of the plate treated in the solution at 80°C also comprised solely the peaks from the substrate (Fig. 4). Moreover, the pattern of the plate immersed in the 40°C solution had higher background than that immersed in the 80°C solution, indicating that the growth of the coating was retarded as the solution temperature was increased form 40 to 80°C.

Cross-sectional TEM characterization.— Figure 5 shows a continuous porous layer formed after 0.5 min of immersion in the solution at 40°C. The light-gray region (indicated by the arrow) between the porous layer and the substrate was also identified as the magnesium substrate, and was likely due to the wedge shape associated with the cross-sectional TEM specimen. As the immersion was continued to 2 min, a relatively thick coating was observed and consisted of two layers: a porous layer contacting the substrate and a cellular overlay as the major layer, as marked by 1 and 2 in Fig. 6a. The cellular layer, once observed, was significantly thicker than the porous layer and showed a quite different overall morphology from the porous layer. Nevertheless, these two layers had a similar composition. Both consisted of oxygen, phosphorus, magnesium, manganese, and aluminum species (Fig. 6b and c). These figures also show that the porous layer contained more aluminum and less manganese than the cellular layer. It was also noted that both the porous layer on the plates after 0.5 and 2 min of immersion had similar morphology, composition, and thickness. This suggests that upon immersion, the porous layer presumably formed via the direct contact of the substrate and solution. Because the light-contrast areas residing in between two conjunctive columns in the cellular layer were mainly the M-Bond epoxy used for sandwiching the two plates together for TEM sample preparation, they could provide pathways for the transportation of the reaction species in the solution to the surface of the porous layer. These reaction species can then diffuse through the porous layer to the coating/substrate interface.

Figure 7a shows the microstructure of the coating formed after 1 min of immersion in the solution at 80°C. The coating was also composed of two layers. The layer intimately contacting the substrate exhibited a compact structure and was identified as magnesium oxide, as illustrated by the inset selective area diffraction (SAD) pattern (lower left corner in Fig. 7a). The interplanar spacing associated with each ring of the SAD pattern is listed in Table I, which matches with those of magnesium oxide. Figure 7a also shows that the layer covering the magnesium oxide layer was rather porous. The inset SAD pattern on the upper-right corner in Fig. 7a contained diffused halos, indicating that this layer was amorphous. In addition to magnesium and oxygen, significant phosphorus and,

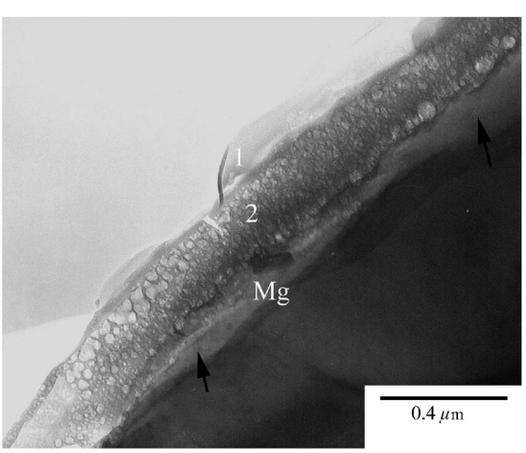

Figure 5. Cross-sectional TEM micrograph of AZ31 plate after 0.5 min of immersion in the phosphate/permanganate solution at 40°C. Areas marked as 1 and 2 are the M-Bond epoxy and the porous layer, respectively.

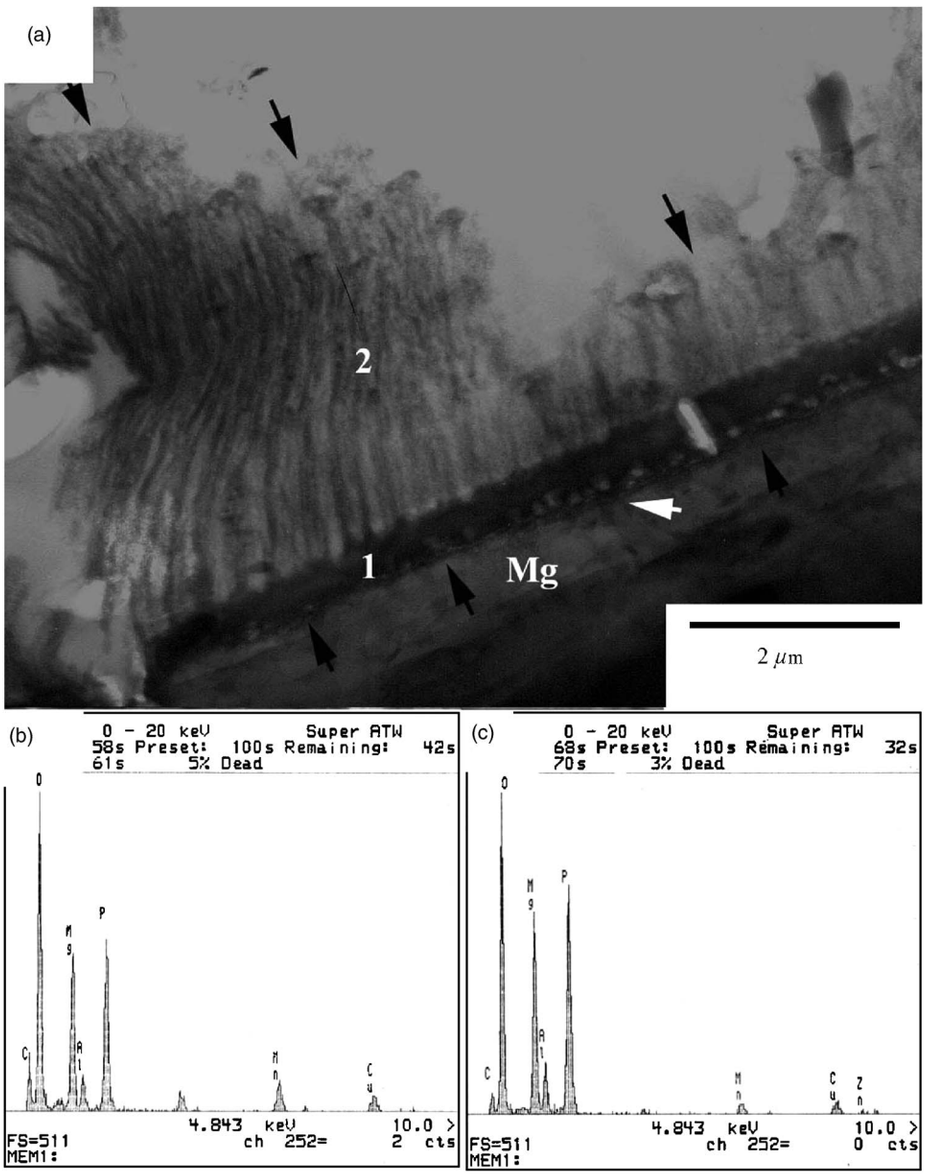

Figure 6. Cross-sectional TEM characterization of AZ31 plate after 2 min of immersion in the phosphate/permanganate solution at 40°C: (a) bright-field image; (b) and (c) are the EDS spectra taken from the cellular layer and the porous layer, respectively. The white arrow indicates the coating/substrate interface.

to a lesser extent, aluminum signals were also detected in the porous layer (Fig. 7b). Furthermore, V-shaped microcracks were frequently observed, as marked by the double arrows in Fig. 7a. They generally had a larger opening near the surface and a sharp tip at the boundary between the porous and magnesium oxide layers.

Thickness of the coating.— As measured on the TEM micrographs, the thickness of the conversion coating was taken as the distance between the coating/substrate interface and coating/M-Bond interface, as marked by a pair of arrows in Fig. 6 and 7, respectively. Since the thickness of the coating might vary from place to place (Fig. 6), the thickness was herein reported as an average of more than ten measurements on several micrographs. Figure 8 shows the thickness of the coating as a function of the immersion time. Regardless of the solution temperature, the growth rate of the coating decreased with continued immersion. This is in good consistence with the dependence of coating thickness on the immersion time for the conversion coating on magnesium.[9,19] Figure 8 also illustrates that the growth rate markedly decreased with increasing solution temperature. Furthermore, the coating formed in the 80°C solution presumably stopped growing after 5 min of immersion, while the coating formed in the 40°C solution continued to grow up to the maximum immersion time studied, i.e., 10 min.

Discussion

Formation of the phosphate/permanganate coating at 40°C.— It has been shown that magnesium alloys treated in a phosphate/permanganate solution at 40 or 50°C display corrosion protective properties comparable to those treated in the chromate solution.[9,11,12] Understanding the formation mechanism of the coating in the phosphate/permanganate solution at 40°C is, therefore, of immense importance. Immersed in acid solutions, for instance pH 3.5 in the present study, the AZ31 plate dissolves immediately in the phosphate/permanganate bath upon immersion and allows an aqueous layer enriched with Mg^{2+}, Al^{3+} to form on the plate surface. Accompanying this oxidation reaction, potential reduction reactions are discharge of protons and reduction of MnO_4^- to Mn^{2+} in acid aqueous solutions (Reaction 1).[21]

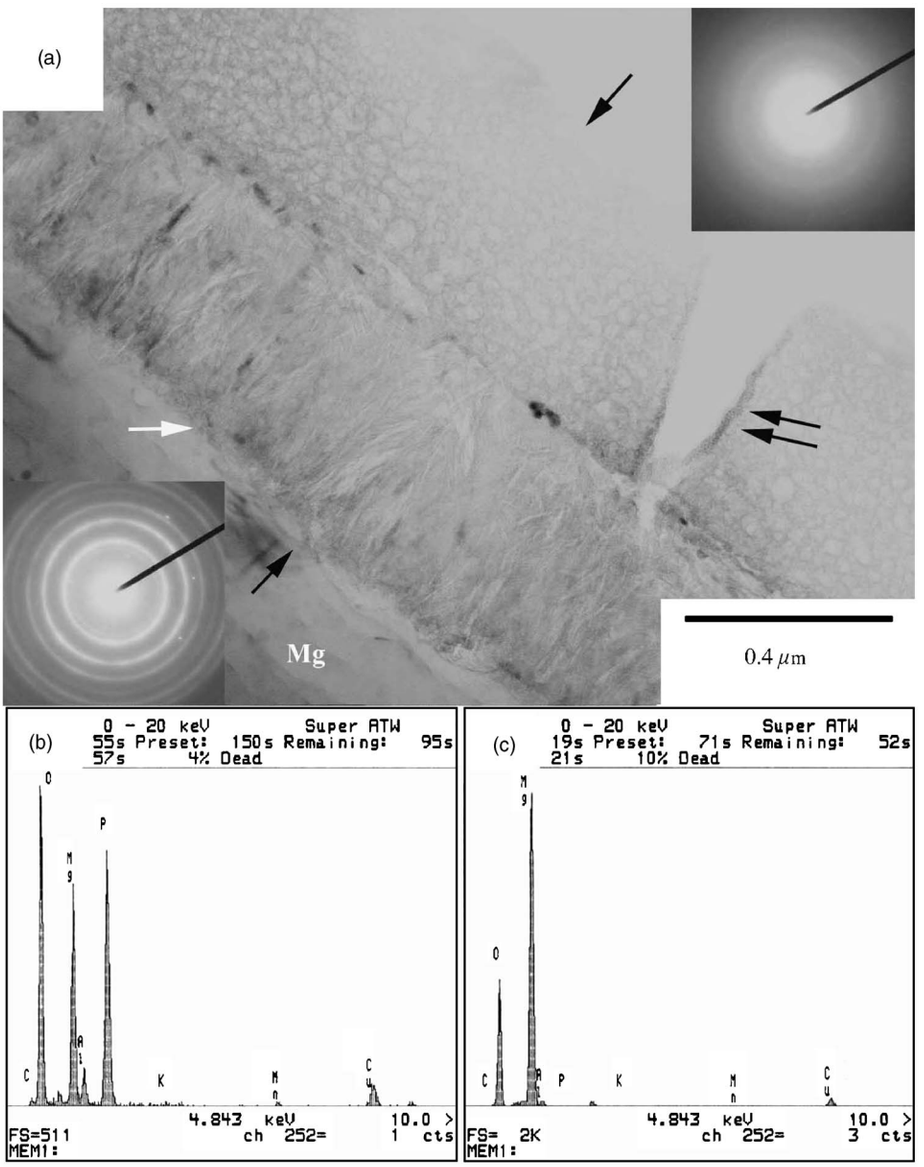

Figure 7. Cross-sectional TEM characterization of AZ31 plate after 1 min of immersion in the phosphate/permanganate solution at 80°C: (a) bright-field image and diffraction patterns; (b) and (c) are the EDS spectra taken from the porous layer and the compact oxide layer, respectively. The white arrow indicates the interface between the magnesium oxide layer and the substrate.

$$MnO_4^- + 8H^+ + 5e^- \rightarrow Mn^{2+} + 4H_2O \quad [1]$$

Proton discharge can create a high-pH environment for the precipitation of various metal hydroxides and phosphates in which magnesium hydroxide and phosphate are the major constituents. As a result of the increase in pH, MnO_4^- can also be reduced to form manganese oxide in neutral or alkaline solution (Reaction 2).[11,21]

$$MnO_4^- + 4H^+ + 3e^- \rightarrow MnO_2 + 2H_2O \quad [2]$$

Manganese oxide can be potentially incorporated into the conversion coating. In fact, the introduction of manganese oxide in the phosphate/permanganate coating has been considered to enhance the corrosion resistance of the coating.[9-12] Therefore, the porous layer that mainly contained oxygen, phosphorus, magnesium, aluminum, and manganese species, can be composed of hydroxides and phosphates of magnesium, aluminum, and manganese, as well as manganese oxide. The porous layer is schematically shown in Fig. 9 illustrating a possible phosphate/permanganate coating evolution on magnesium in the 40°C solution. The porous layer might protect the substrate from direct attack by the solution. Its porous nature, however, can facilitate the coating formation via the transportation of

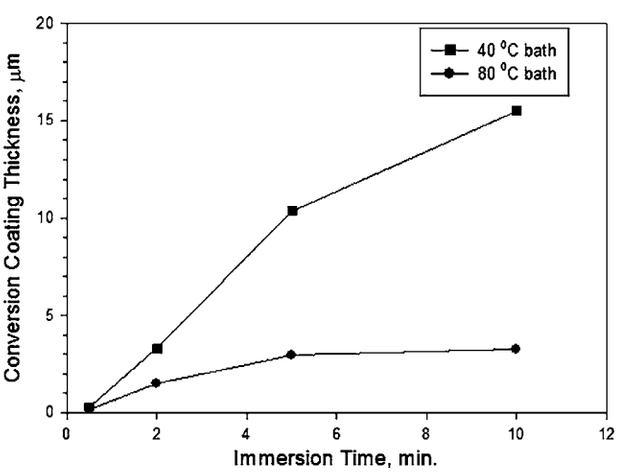

Figure 8. Thickness of the conversion coating as a function of immersion time.

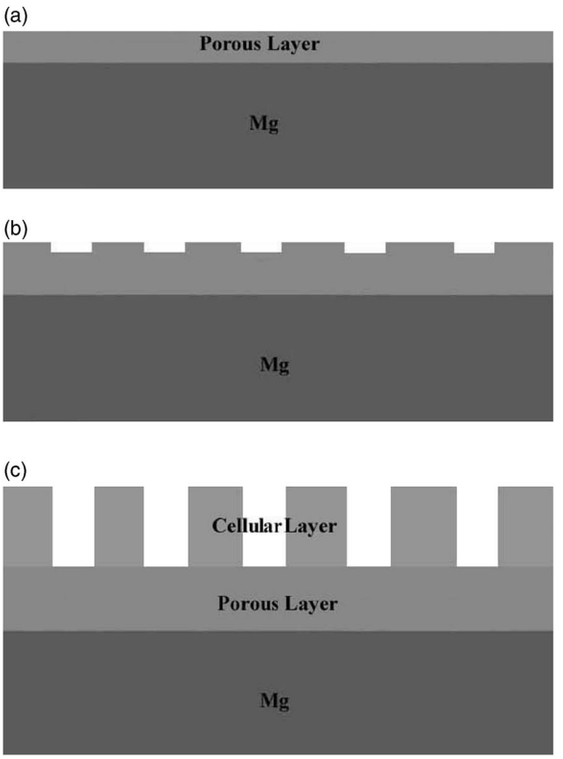

Figure 9. A possible schematic representation illustrating the evolution of porous inner layer and cellular overlay on AZ31 plate immersed in the phosphate/permanganate solution at 40°C.

reaction ions and solution through this porous layer. Therefore, the growth of the coating continues as the immersion proceeds (Fig. 8).

Together with hydrogen discharge, a recovery of proton concentration at the coating/solution interface can occur via proton diffusion in the solution. Furthermore, the strong oxidation ability associated with MnO_4^- can cause oxidation of water to form oxygen and proton (Reaction 3).

$$2H_2O \rightarrow O_2 + 4H^+ + 4e^- \quad [3]$$

This oxidation reaction results in more protons near the interface between the porous layer and the solution. Increase in acidity can cause local dissolution of the porous layer because both the hydroxide/oxide and phosphate of magnesium and manganese are not stable species in acid media.[11,21] This local dissolution results in the breakdown of the planar interface between the porous layer and the solution. As a result, a cellular morphology evolves at the coating/solution interface (Fig. 9b). Meanwhile, the substrate is continuously attacked by the solution transported through the porous layer. The porous layer will then grow into the substrate, while dissolution continues at the interface between the porous layer and the cellular layer. This results in the thinning of the porous layer, but the growth of the cellular layer (Fig. 9c). The growth rate, however, decreases as the immersion continues. This can be due to the increase in the length of the pathway for transporting the reaction species from the solution to the porous/cellular interface with continued immersion.

Effect of solution temperature.— Magnesium in the aqueous solution with pH exceeding 8.5 can be passivated by the formation of magnesium hydroxide, but not by magnesium oxide.[21] This is because the enthalpy of formation for magnesium hydroxide and oxide at 25°C is −142 580 and −136 130 cal/g-mole, respectively. Indeed, magnesium hydroxides precipitate and deposit on the substrate in the phosphate/permanganate solution at 40°C. Instead of magnesium hydroxide, a magnesium oxide layer forms and intimately contacts the magnesium substrate in the solution at 80°C. It is not immediately clear as to why magnesium oxide instead of hydroxide forms in this 80°C solution. The dehydration of magnesium hydroxide or the direct oxidation of magnesium in the presence of oxygen in the solution, however, can lead to the formation of magnesium oxide.

Table I. Interplanar spacing associated with the diffraction pattern in the lower left corner of Fig. 7a and magnesium oxide, respectively.

Interplanar spacing (Å)		
Measured from SAD pattern	MgO[a]	Diffraction plane
2.09	2.106	(200)
1.48	1.489	(220)
1.24	1.270	(311)
1.09	1.053	(400)
0.97	0.9665	(331)
0.88	0.860	(422)

[a] JCPDS file no. 04-0829.

First, the magnesium oxide can form via the formation of magnesium hydroxide and its subsequent dehydration, as shown by Reactions 4 and 5, respectively.

$$Mg^{2+} + 2H_2O \rightarrow Mg(OH)_2 + 2H^+ \quad [4]$$

$$Mg(OH)_2 \rightarrow MgO + H_2O \quad [5]$$

Because Reaction 5 is an endothermic reaction, increasing temperature favors the formation of magnesium oxide. During the electrodeposition of zinc oxide in a zinc perchlorate solution, it has been shown that ZnO is deposited via dehydration of $Zn(OH)_2$ when the solution temperature exceeds 50°C.[22]

Second, magnesium oxide can form via the direct oxidation of magnesium in the present of oxygen in the solution (Reaction 6).

$$2Mg + O_2 \rightarrow 2MgO \quad [6]$$

According to Reaction 3, in the presence of MnO_4^-, water can be oxidized to form oxygen and proton. If increasing solution temperature enhances the oxidization ability associated with MnO_4^- in aqueous solutions, magnesium oxide, instead of hydroxide, can form directly on the surface of the magnesium substrate.

As the immersion proceeds, the proton concentration at the oxide layer/solution interface will increase gradually due to either the proton diffusion in the solution or the oxidization of water. Finally, the oxide layer dissolves and the porous overlay forms. The presence of compact magnesium oxide effectively prevents the direct attack of the substrate by the solution. Hence, the growth of the coating is retarded.

Conclusions

This study investigated the microstructure and growth behavior of phosphate/permanganate conversion coating on AZ31 magnesium alloy. After 0.5 min of immersion in the solution at 40°C, a porous layer formed and intimately contacted the magnesium substrate. Increasing the immersion time to 2 min resulted in the coating composed of two layers: a porous layer contacting the substrate and a cellular overlay. Both layers comprised magnesium, aluminum, manganese, oxygen, and phosphorus species. The coating continued to grow at a decreasing rate with continued immersion. The coating formed in the solution at 80°C also exhibited a two-layered structure, in which a compact magnesium oxide layer was observed to reside in between the magnesium substrate and a porous layer as the

major overlay. The compact magnesium oxide layer effectively prevented the substrate from direct attack by the solution, thus significantly reducing the growth rate of the coating.

The coating formed in the solution at 40°C results from a dissolution/precipitation mechanism. The dissolution of the substrate leads to the formation of the porous layer contacting the substrate, while local dissolution of the porous layer causes nucleation and growth of the cellular layer. Finally, the formation of magnesium oxide layer in the 80°C solution can be attributed to dehydration of magnesium hydroxide or the direct oxidation of magnesium in the presence of oxygen in the solution.

Acknowledgments

The authors would like to thank the National Science Council, Republic of China, for financially supporting this research under grant no. 922216E002017. L. C. Wang, National Sun Yat-sen University, is acknowledged for her assistance with the TEM work. This study made use of the Electron Microscopes of National Taiwan University and National Sun Yat-sen University, supported by the National Science Council, Republic of China.

National Taiwan University assisted in meeting the publication costs of this article.

References

1. T. Biestek and J. Weber, *Electrolytic and Chemical Conversion Coatings*, 1st ed., Portcullis Press Ltd., Redhill, Surrey, UK (1976).
2. J. E. Gray and B. Luan, *J. Alloys Compd.*, **336**, 88 (2002).
3. Yu. Simaranov, A. I. Marshakov, and Yu. N. Mikhailovskii, *Prot. Met.*, **25**, 611 (1990).
4. M. W. Kendig, A. J. Davenport, and H. S. Issacs, *Corros. Sci.*, **34**, 41 (1993).
5. S. M. Cohen, *Corrosion*, **51**, 71 (1995).
6. L. Xia and R. L. McCreery, *J. Electrochem. Soc.*, **145**, 3083 (1998).
7. W. R. McGovern, P. Schmutz, R. G. Buchheit, and R. L. McCreery, *J. Electrochem. Soc.*, **147**, 4494 (2000).
8. Y. Liu, P. Skeldon, G. E. Thompson, H. Habazaki, and K. Shimizu, *Corros. Sci.*, **46**, 297 (2004).
9. D. Hawke and D. L. Albright, *Met. Finish.*, **93**, 34 (1995).
10. H. Umehara, S. Terauchi, and M. Takaya, *Mater. Sci. Forum*, **350–351**, 273 (2000).
11. H. Umehara, M. Takaya, and Y. Kojima, *Mater. Trans.*, **42**, 1691 (2001).
12. K. Z. Chong and T. S. Shih, *Mater. Chem. Phys.*, **80**, 191 (2003).
13. M. A. Gonzalez-Nunez, P. Skeldon, G. E. Thompson, and H. Karimzadeh, *Corrosion*, **55**, 1136 (1999).
14. M. A. Gonzalez-Nunez, C. A. Nunze-Lopez, P. Skeldon, G. E. Thompson, H. Karimzadeh, P. Lyon, and T. E. Wilks, *Corros. Sci.*, **37**, 1763 (1995).
15. C. S. Lin, H. C. Lin, K. M. Lin, and W. C. Lai, *Corros. Sci.*, **48**, 93 (2006).
16. A. L. Rudd, C. B. Breslin, and F. Mansfeld, *Corros. Sci.*, **42**, 275 (2000).
17. M. Dabalà, K. Brunelli, E. Napolitani, and M. Magrini, *Surf. Coat. Technol.*, **172**, 227 (2003).
18. K. Brunelli, M. Dabalà, I. Calliari, and M. Magrini, *Corros. Sci.*, **47**, 989 (2005).
19. C. S. Lin and S. K. Fang, *J. Electrochem. Soc.*, **152**, B54 (2005).
20. M. P. Schriever, Canadian Pat. 2056159 (1990).
21. M. Pourbaix, *Atlas of Electrochemical Equilibria in Aqueous Solutions*, 2nd ed., NACE, Houston, TX (1974).
22. Th. Pauporte and D. Lincot, *J. Electrochem. Soc.*, **148**, C310 (2001).